HAL
open science

TGFBI secreted by mesenchymal stromal cells ameliorates osteoarthritis and is detected in extracellular vesicles

Maxime Ruiz, Karine Toupet, Marie Maumus, Pauline Rozier, Christian Jorgensen, Danièle Noël

To cite this version:

Maxime Ruiz, Karine Toupet, Marie Maumus, Pauline Rozier, Christian Jorgensen, et al.. TGFBI secreted by mesenchymal stromal cells ameliorates osteoarthritis and is detected in extracellular vesicles. Biomaterials, 2020, 226, pp.119544. 10.1016/j.biomaterials.2019.119544 . hal-02329519

HAL Id: hal-02329519

https://hal.umontpellier.fr/hal-02329519v1

Submitted on 23 Oct 2019

HAL is a multi-disciplinary open access archive for the deposit and dissemination of scientific research documents, whether they are published or not. The documents may come from teaching and research institutions in France or abroad, or from public or private research centers.

L'archive ouverte pluridisciplinaire **HAL**, est destinée au dépôt et à la diffusion de documents scientifiques de niveau recherche, publiés ou non, émanant des établissements d'enseignement et de recherche français ou étrangers, des laboratoires publics ou privés.

Manuscript
Click here to download Manuscript: TGFBI MSC CIOA-main-revised.docx Click here to view linked References

TGFBI secreted by mesenchymal stem cells ameliorates osteoarthritis and is detected in extracellular vesicles

Maxime Ruiz[a], Karine Toupet[a], Marie Maumus[a], Pauline Rozier[a], Christian Jorgensen[a,b,*], Danièle Noël[a,b,*]

[a]IRMB, Univ Montpellier, INSERM, CHU Montpellier, Montpellier, France; [b]Hôpital Lapeyronie, Clinical immunology and osteoarticular diseases Therapeutic Unit, Montpellier, France.

*: equally contributing authors

Corresponding author:

D. Noël, Inserm U1183, IRMB, Hôpital Saint-Eloi,

80 avenue Augustin Fliche, 34295 Montpellier cedex 5, France

Tel: +33 4 67 33 04 73 – Fax: +33 4 67 33 01 13 – E-mail: daniele.noel@inserm.fr

ABSTRACT

Mesenchymal stem/stromal cells (MSCs) are of interest in the context of osteoarthritis (OA) therapy. We previously demonstrated that TGFβ-induced gene product-h3 (TGFBI/BIGH3) is downregulated in human MSCs (hMSCs) from patients with OA, suggesting a possible link with their impaired regenerative potential. In this study, we investigated TGFBI contribution to MSC-based therapy in OA models. First, we showed that co-culture with murine MSCs (mMSCs) partly restored the expression of anabolic markers and decreased expression of catabolic markers in OA-like chondrocytes only upon priming by TGFβ3. Moreover, TGFβ3-primed hMSCs not only modulated the expression of anabolic and catabolic markers, but also decreased inflammatory factors. Then, we found that upon TGFBI silencing, mMSCs partly lost their inductive effect on chondrocyte anabolic markers. Injection of hMSCs in which TGFBI was silenced did not protect mice from OA development. Finally, we showed that MSC chondroprotection was due to the presence of TGFBI mRNA and protein in extracellular vesicles. Our findings suggest that TGFBI is a chondroprotective factor released by MSCs and an anabolic regulator of cartilage homeostasis.

Keywords: mesenchymal stem cells, TGFBI, osteoarthritis, cartilage, chondrocyte, extracellular vesicle

INTRODUCTION

Mesenchymal stem/stromal cells (MSCs) are multipotent progenitor cells that are primarily isolated from bone marrow and adipose tissue, but that can also be found in many other tissues, including umbilical cord and deciduous teeth [1]. These fibroblastic-like adherent cells are characterized by a panel of positive and negative markers and the potential to differentiate into the three mesenchymal lineages [2]. MSCs also secrete many factors that act in a paracrine fashion and play important roles in their therapeutic effect [3]. Recent findings indicate that most of these factors are conveyed by extracellular vesicles (EVs) that take part in intercellular communication by acting as vehicles for the transfer of mediators between cells [4]. Previous studies on factors that mediate *in vivo* the beneficial function of MSCs showed that interleukin 6 (IL6), IL1 receptor antagonist, and glucocorticoid induced leucine zipper are anti-inflammatory mediators in experimental arthritis, whereas thrombospondin-1 is a chondroprotective factor in osteoarthritis (OA) [5-8]. Nevertheless, the identification of factors responsible for MSC clinical benefit in rheumatic diseases is still incomplete.

OA is the most common rheumatic disease. Its prevalence increases with age, and is higher in patients with metabolic syndromes or obesity [9]. OA is characterized by progressive cartilage destruction, but it also affects all other joint tissues, leading to sub-chondral bone sclerosis, synovium inflammation and fat pad fibrosis [10, 11]. In patients with severe forms, it results in the loss of joint function, pain and functional disability. Currently, there is no curative treatment and the available pharmaceutical options only alleviate symptoms, such as pain and inflammation. In patients with advanced OA, joint replacement surgery offers pain relief and restores function and mobility. Recent studies have evaluated the interest of delivering MSCs in

the pathological joint, as a possible innovative therapeutic solution. MSC chondroprotective effect has been demonstrated in preclinical models of OA [12-14], and the safety and efficacy of this approach are now evaluated in the clinic (for review, see [15]). Both allogeneic and autologous MSCs are used; however, questions have been raised on the efficacy of MSCs isolated from aged donors or with age-associated diseases [16]. Indeed, MSCs from aged donors show reduced proliferative capacity, differentiation potential, and migration as well as increased senescence [17]. As MSCs adapt and respond to their microenvironment, a pathological state might perturb the stem cell niche where MSCs reside. Therefore, the interactions between MSCs and their niche will result in modifications of their secretome. For instance, several factors secreted in the joint environment, particularly members of the transforming growth factor-β (TGFβ) family [18], are deregulated in OA and contribute to the breakdown of cartilage homeostasis. At basal levels, TGFβ signalling contributes to cartilage homeostasis. On the other hand, high concentrations of TGFβ are found in the synovial fluids of patients with OA [19]. Interestingly, deregulation of TGFβ signalling in MSCs is involved in OA onset or progression, and knock out of TGFβ type II receptor in MSCs attenuates cartilage erosion and subchondral bone sclerosis [20]. We recently reported that TGFβ-induced gene product-h3 (TGFBI/BIGH3/RGD-CAP) is upregulated in cartilage and bone from patients with OA, whereas it is downregulated in bone marrow-derived human MSCs (hMSCs) [21]. We also found that TGFBI downregulation in hMSCs partly compromises their chondrogenic potential. Therefore, we hypothesized that TGFBI downregulation in hMSCs from patients with OA may affect their functional properties and impair their regenerative/repair potential. Here, we investigated whether TGFBI deregulation in OA affects MSC chondroprotective role.

MATERIALS AND METHODS

Mesenchymal stem cell culture. Human specimens were recovered from patients with OA undergoing knee replacement surgery after written informed consent, in accordance with the Declaration of Helsinki. The study was carried out following the recommendations by the Languedoc-Roussillon Committee for the Protection of Persons and was approved by the French Ministry of Higher Education and Research (DC-2010-1185). After isolation from bone marrow, hMSCs were characterized by phenotyping and tri-lineage differentiation, as described [22]. They were cultured in proliferative medium [αMEM, 2 mmol/mL glutamine, 100 µg/mL penicillin/streptomycin, 10% foetal calf serum (FCS), and 1 ng/mL basic fibroblast growth factor (bFGF) (R&D Systems, Lille)], and used between passage 2 and 5. Murine MSCs (mMSCs) were isolated from bone marrow of C57BL/6 mice, expanded in proliferative medium, and characterized as previously reported [5]. They were used between passage 12 and 20.

EV isolation and characterization. EVs were isolated from conditioned supernatants of mMSCs (mMSC-EVs) by differential ultracentrifugation to recover large-size EVs and small-size EVs at 18 000 and 100 000 g, respectively. EVs were characterized following the guidelines provided by the International Society of Extracellular Vesicles (ISEV), as already described in [23]. Similar protocols were used for the production and isolation of hMSC-EVs. Briefly, hMSCs (10^6/dish) were cultured in proliferative medium with 3% EV-free FCS for 60h for production of EV-rich supernatant. Total EVs, which contain small-size and large-size EVs, were isolated according to the described protocol [23]. EV characterization included the determination of size

and concentration by nanoparticle tracking analysis (NanoSight LM10-12 Malvern Instruments, Orsay), protein quantification with the Micro BCA Protein Assay Kit (Pierce, ThermoFisher Scientific, Illkirsch), and surface marker detection (anti-CD81 from Miltenyi Biotech, Paris; and anti-CD44, -CD63, CD73, -CD90, -CD105 antibodies from BD Biosciences, Le Pont de Claix) on EV-coated beads, as described [23].

Cartilage explant and chondrocyte culture. Femoral heads were dissected from 2-week-old C57BL/6 mice as described [24]. After 72h of stabilization in proliferative medium, OA-like changes were induced in cartilage explants by culture in serum-free medium with 10 ng/mL IL-1β (R&D Systems) for another 72h. Thereafter, OA-like explants were co-cultured with $2x10^5$ mMSCs seeded in polyethylene terephthalate culture inserts with 0.4 µm pore size (BD, Corning, Boulogne-Billancourt) for 24h.

Murine articular chondrocytes were isolated from the knees and femoral heads of 3-day-old C57BL/6 mice, as described [25]. Chondrocytes were plated (25 000cells/cm^2) in 12-well TPP culture plates (TPP Techno Plastic Products, Switzerland) with 1mL of proliferative medium for 5 days. Thereafter, OA-like chondrocytes were induced by incubation with 1 ng/mL IL-1β (R&D Systems) for 24h (day 0). In parallel, mMSCs were cultured in 1mL of proliferative medium in 12-well culture plates. At 80% confluence, they were primed (or not) with 10 ng/mL TGFβ3 (R&D Systems) for 24h, then rinsed twice with PBS, and cultured for 24h to obtain conditioned medium (mMSC-CM). mMSC-CM (1mL/well) was then added to OA-like chondrocytes for 24h (day 1) before recovering chondrocytes for RT-qPCR analysis.

For co-culture with mMSCs or hMSCs, $2x10^5$ OA-like chondrocytes were seeded in 12-well culture inserts with 1mL of proliferative medium and primed (or not) with 10 ng/mL TGFβ3 for 24h. After two washes with PBS, mMSC- or hMSC-containing inserts were added to OA-like chondrocytes on day 0 with fresh medium and co-cultured for 24h (day 1). Chondrocytes were recovered and processed for RT-qPCR.

Glycosaminoglycan (GAG) content measurement. GAG content was measured using the Blyscan Glycosaminoglycan Assay according to the supplier's recommendations (Biocolor Ltd, UK). Supernatants from OA-like explants were collected and cultured OA-like explants were digested overnight with 125 µg/mL papain (Sigma) in sodium acetate buffer (0.1M; pH=5.5) containing 5mM EDTA and 5mM L-cysteine HCl. Supernatants and digestion products were diluted to fit the calibration curve. Colorimetric values were obtained using a Varioskan LUX microplate reader.

Cell transfections. At 60% confluence, mMSCs and hMSCs were transfected with 50nM of siRNA-control (siCT), siRNA-mTGFBI or siRNA-hTGFBI (siTGFBI) (Ambion, ThermoFisher Scientific) using the Oligofectamine reagent and according to the supplier's recommendations (Life Technologies, Courtaboeuf). Chondrocytes were transfected with 400nM of each siRNA using the Lipofectamine reagent, according to the supplier's recommendations (Life Technologies, Courtaboeuf). Cells were used 48h after transfection.

Proliferation and adhesion assays. For both assays, 96-well TPP plates were coated with 10 µg/mL recombinant human TGFBI (rhTGFBI; R&D Systems) and incubated at 4°C overnight. Then, wells were washed twice with PBS and blocked with 2% BSA at room temperature for 1h. For proliferation assays, $2x10^4$ murine chondrocytes were seeded on rhTGFBI-coated plates and incubated for 72h. For adhesion assays, $5x10^4$ murine chondrocytes were seeded on rhTGFBI-coated plates and after 2h, 4h, and 6h, wells were washed twice with PBS to remove non-adherent cells before quantification of the adhering cells. Cell number was quantified by measuring cell viability using the CellTiter-Glo luminescent assay (Promega, Charbonnières-les-Bains), according to the manufacturer's protocol. Cell numbers were estimated relative to a standard curve generated using 10-fold serial dilutions of chondrocytes and the cell number in non-treated wells was set to 1.

Splenocyte proliferative assay. Splenocytes were isolated from C57Bl6 mice and cultured with hMSCs transfected with siCT or siTGFBI, as described [8]. After 3 days of incubation, splenocyte proliferation was assessed using the CellTiter-Glo Luminescent Cell Viability Assay (Promega, Charbonnières-les-Bains) following the manufacturer's instructions. Splenocyte proliferation was quantified by subtracting the signal of unstimulated splenocytes, and calculated as the percentage of the value obtained in concanavalin A-stimulated splenocytes (100%).

RNA extraction and RT-qPCR. Total RNA was isolated from h/mMSCs or chondrocytes using the RNeasy kit according to the supplier's protocol (Qiagen, Courtaboeuf); from cartilage and

bone with 0.1 mL TRIzol reagent (ThermoFisher Scientific)/g tissue, followed by chloroform and phenol acid extraction; and from EVs using the miRNeasy Micro Kit (Qiagen). Total RNA (0.5 µg) was reverse transcribed using 100 U of M-MLV reverse transcriptase (ThermoFisher Scientific), and PCR reactions were performed as described [26]. Primer sequences (SYBR Green Technologies) are described in Table 1. All values were normalized to the *RPS9* housekeeping gene, and expressed as relative expression or fold change using the respective formulae: $2^{-\Delta CT}$ and $2^{-\Delta\Delta Ct}$. For EVs, gene expression was quantified in 10 ng of cDNA and normalized to the Ct values.

Collagenase-induced osteoarthritis model. The collagenase-induced OA (CIOA) model was generated in accordance with the guidelines and regulations of the Ethical Committee for animal experimentation of the Languedoc-Roussillon region (Approval APAFIS#5349-2016050918198875). Experiments were performed after the final approval by the French Ministry for Education, Higher Education and Research. OA was induced by two injections (day 0 and 2) of 1U type VII collagenase in 5 µL saline in the intra-articular (IA) space of one hind knee joint in 10-week-old C57BL/6 mice. Then, groups of 23 mice received or not IA injections of siCT- or siTGFBI-transfected hMSCs ($2.5x10^5$ cells/5 µL saline) at day 7. Mice were euthanatized at day 42 and hind paws were fixed in 4% formaldehyde for further analysis.

Bone parameter analysis. Hind paws were scanned in a SkyScan 1176 micro-CT scanner (Bruker, Belgium) using the following parameters: 0.5 mm aluminium filter, 45 kV, 500 µA, resolution of 18 µm, 0.5° rotation angle. Scans were reconstructed using the NRecon software

(Bruker). Misalignment compensation, ring artefacts and beam-hardening were adjusted to obtain the correct reconstruction of each paw. Bone degradation was quantified in subchondral bone of the medial plateau for each tibia (CTAn software, Bruker). Calcification of the lateral and medial meniscal/external ligaments and osteophyte formation on joint edges were also quantified. 3D images of joints were reconstructed using the Avizo software (Avizo Lite 9.3.0, FEI Visualization Sciences Group, Lyon, France).

Confocal laser scanning microscopy. A confocal laser scanning microscope (CLSM; TCS SP5-II, Leica Microsystems, Nanterre) was used to acquire images of the medial tibial plateau articular cartilage. Articular cartilage was scanned in depth (XYZ-mode) using the following parameters: voxel size 6 µm, 5x dry objective, and UV laser light source (405 nm). Image stacks were used to reconstruct a 3D image of the medial tibial plateau cartilage and then to quantify cartilage morphometric parameters using the Avizo software.

Histological analysis. Hind paws were decalcified in 5% formic acid solution for 2 weeks, and then processed for paraffin embedding. Coronal sections of tibias were cut (3 slices of 7 µm each 100 µm; first section at 50 µm below the cartilage surface) and stained with Safranin O/Fast Green. Cartilage degradation was quantified using the modified Pritzker OARSI score, as described [27]. Osteophyte size at the edges of the tibia cartilage was scored using an arbitrary score from 0 to 3, as described [14].

Statistical analysis. Statistical analysis was performed with the GraphPad Prism software. Each sample/cell was independent and represented an experimental unit providing a single outcome. The data normal distribution and variance homogeneity were determined with the Shapiro-Wilk and Fisher's exact tests (2 groups) or the Bartlett's test (>2 groups), followed by the appropriate tests, as detailed in each figure legend. Data are presented as the mean ± SEM with $p<0.05$ (*), $p<0.01$ (**), $p<0.001$ (***).

RESULTS

TGFBI is deregulated in OA-like femoral head explants and chondrocytes. We previously showed by immunohistochemistry that TGFBI is upregulated in the cartilage from patients with OA and in CIOA mice compared with healthy controls [28]. To better understand the effect of TGFBI deregulation, we first evaluated its expression by RT-qPCR in mice at different ages. We found that *TGFBI* mRNA expression was higher in cartilage than in cortical bone or bone marrow in healthy 3-day-old mice (Fig. 1A). *TGFBI* expression was also higher in the femoral heads of adult mice compared with cortical bone or total bone marrow, and in tibial epiphyses compared with bone marrow (Fig. 1B). This suggests higher expression in cartilage-containing tissues. Importantly, *TGFBI* mRNA levels tended to be higher in tibial epiphyses from CIOA mice than in healthy controls, confirming TGFBI upregulation in OA joint tissues (Fig. 1C). We next determined whether OA-related TGFBI deregulation can be reproduced in *in vitro* models. First, we demonstrated that mouse femoral head explants (Fig. 1D) cultured with IL1β reproduced the OA-like cartilage phenotype, as indicated by the downregulation of the anabolic markers

type IIB collagen (*Col2a1*) and aggrecan (*Acan*) and the upregulation of the catabolic markers matrix metalloproteinase 13 (*Mmp13*) and A Disintegrin And Metalloproteinase with Thrombospondin Motifs 5 (*Adamts5*) (Fig. 1E). In addition, IL1β significantly increased GAG release in the culture supernatant, and decreased GAG content in cartilage explants. Moreover, *Tgfbi* level was higher in OA-like explants compared with untreated controls (Fig. 1E).

Similarly, immature articular chondrocytes isolated from neonatal mice displayed an OA-like phenotype after incubation with IL1β (Fig. 1F). Specifically, expression of *Col2a1* and *Acan* was decreased, whereas that of *Mmp13* and *Adamts5* was increased after 24h of incubation with IL1β (Fig. 1G). Moreover, the genes encoding several inflammatory mediators, such as IL6, inducible nitric oxide synthase (iNOS), monocyte chemoattractant protein (MCP)1 and cyclooxygenase (COX)2, were upregulated, whereas tumour necrosis factor (TNF)α remained unchanged. In this model, *Tgfbi* was downregulated (Fig. 1G), indicating a deregulation of TGFBI in both *in vitro* models of OA.

Naive murine and human MSCs cannot normalize the phenotype of OA-like chondrocytes. We then investigated the effect of mMSCs on OA-like femoral head explants (experimental strategy in Fig. 1D). GAG release in the supernatant was decreased and the expression of *Acan* and *Col2a1* was increased in OA-like explants co-cultured with mMSCs compared with explants alone, indicating a chondroinductive effect of mMSCs (Fig. 2A). As femoral head explants are made of several tissues (cartilage, bone and bone marrow), we evaluated the effect of mMSCs specifically on OA-like chondrocytes (experimental strategy in Fig. 1F). Co-culture with mMSCs did not significantly change the expression of anabolic, catabolic and inflammatory factors in

OA-like chondrocytes. Conversely, addition of mMSC-CM increased *Acan* expression, compared with OA-like chondrocytes alone, but without reaching the levels of chondrocytes not exposed to IL1β. The expression of type IIB collagen and of catabolic and inflammatory mediators was not modified by addition of mMSC-CM (Fig. 2B-C). Finally, we evaluated whether co-culture with hMSCs influenced the phenotype of murine OA-like chondrocytes and found no significant change, except for a decrease of iNOS expression (Fig. 2D).

TGFβ3-primed murine and human MSCs reverse the deregulation of cartilage markers in OA-like chondrocytes. As the TGFβ pathway has regulatory functions in cartilage homeostasis (REF) and TGFBI downregulation in OA MSCs impairs their functional properties (REF), we tested whether TGFBI upregulation in MSCs modified their effect on OA-like chondrocytes. We first showed that priming with TGFβ3 upregulated *TGFBI* transcription in mMSCs and hMSCs by 2- and 3-fold, respectively (Fig. 3A-B) and increased TGFBI secretion by 3.5-fold in hMSCs (Fig. 3B, right panel). Moreover, incubation of OA-like mouse chondrocytes with TGFβ3-primed mMSC-CM significantly upregulated the expression of chondrocyte anabolic markers, but did not change the expression of catabolic and inflammatory factors (Fig. 3C). Co-culture of OA-like chondrocytes with TGFβ3-primed mMSCs led to upregulation of anabolic markers and downregulation of catabolic markers, but did not significantly modulate inflammation-associated markers (Fig. 3D). Conversely, co-culture with TGFβ3-primed hMSCs significantly reversed the deregulated expression of all tested markers, including inflammatory mediators (Fig. 3E). Altogether, these results indicated that mMSC pro-anabolic function is regulated by

TGFβ3-priming. However, their anti-catabolic role requires both TGFβ3-priming and co-culture, indicating the importance of the crosstalk with OA-like chondrocytes.

TGFBI silencing in murine MSCs partly impairs their chondroinductive effect on OA-like chondrocytes. We then investigated the effect of TGFBI downregulation in mMSCs after transfection with a siTGFBI that reduced by 33% *Tgfbi* mRNA level compared with siCT (Fig. 4A). This decrease was sufficient to inhibit mMSC chondroinductive effect, as shown by the absence of *Acan* and *Col2a1* upregulation in OA-like chondrocytes co-cultured with siTGFBI-transfected mMSCs compared with siCT-mMSCs (Fig. 4A). Similarly, *Acan* upregulation was slightly but significantly lower in OA-like chondrocytes co-cultured with TGFβ3-primed siTGFBI-mMSCs than with TGFβ3-primed siCT-mMSCs (Fig. 4B). Finally, siTGFBI transfection in hMSCs reduced *TGFBI* expression by 48% (Fig. 4C). However, TGFBI downregulation did not modify the expression of *Acan* and *Col2a1* in OA-like chondrocytes co-cultured with TGFβ3-primed siTGFBI hMSCs.

TGFBI silencing impairs the therapeutic function of human MSCs in CIOA mice. Then, we evaluated *in vivo* the effect of IA injection of siCT- or siTGFBI-transfected hMSCs (TGFBI expression reduced by 70%) in CIOA mice [29]. Histological analysis showed that the OA score was lower, although not significantly, in CIOA mice treated with siCT-hMSCs compared with untreated mice (Fig. 5A-B). Conversely, the score was significantly higher in mice treated with siTGFBI-hMSCs compared with mice treated with siCT-hMSCs and untreated controls. Histomorphometric analysis of cartilage by CLSM confirmed that cartilage degradation was more important, and cartilage thickness was lower in CIOA mice treated with siTGFBI-hMSCs

compared with siCT-hMSCs (Fig. 5C-D). Accordingly, micro-CT analysis showed that sub-chondral bone parameters in CIOA mice treated with siCT-hMSCs were similar to those of healthy mice. Conversely, CIOA mice that received siTGFBI-hMSCs were not protected from bone degradation (Fig. 5E-F). Finally, injection of siCT-hMSCs, but not of siTGFBI-hMSCs partly inhibited calcification of the lateral and medial menisci and ligaments in CIOA mice (Fig. 5G-H). Overall, these findings indicated that TGFBI produced by hMSCs contributes to their therapeutic effect in CIOA mice.

TGFBI is conveyed within MSC-derived extracellular vesicles. To understand TGFBI mechanism of action, we assessed its effect on chondrocyte functions. Addition of rhTGFBI enhanced the proliferation of murine chondrocytes, while culture in rhTGFBI-coated dishes reduced chondrocyte adhesion (Fig. 6A-B). Moreover, splenocyte proliferation was slightly, but significantly reduced by siTGFBI-transfected hMSCs, suggesting decreased immunosuppressive properties upon TGFBI silencing (Fig. 6C). Then, we asked whether TGFBI could be conveyed by MSC-EVs that have been shown to have immunomodulatory effects in an arthritis model [23] and to transfer MSC-secreted factors between cells [4]. Using an already validated protocol for mMSC-EVs, we isolated and characterized total EVs from hMSCs [23]. The quantity of hMSC-EVs was $8x10^8$ particles/µg total proteins/10^6 hMSCs, and their size ranged from 80 to 400 nm (Fig. 6D). They expressed surface markers of hMSCs (CD44, CD73, and CD90) and of exosomes (CD63 and CD81) (Fig. 6E). We detected easily quantifiable amounts of TGFBI protein in hMSC-EVs, although the amounts were lower than in hMSCs (Fig. 6F). We also detected *TGFBI* mRNA in hMSC-EVs and in small-size and large-size mMSC-EVs (Fig. 6G-H).

DISCUSSION

This is the first evidence that TGFBI produced by hMSCs exerts a pro-anabolic function on chondrocytes and a therapeutic role in OA by preventing cartilage and bone degradation, while inhibiting soft tissue calcification.

Using two *in vitro* models that mimic the cartilage degradation and chondrocyte deregulation observed in OA, we revealed TGFBI expression deregulation in OA-like cartilage. Specifically, TGFBI was upregulated in OA-like femoral head explants, while it was downregulated in OA-like chondrocytes. A possible explanation for this discrepancy might be related to the developmental stage of the analysed tissues. In femoral head explants from 2-3-week-old mice, TGFBI expression is typical of the adult age, and increases in OA-like conditions as observed in epiphyses of CIOA-induced adult mice. This upregulation might be related to a regulatory loop to inhibit cartilage mineralization that occurs during OA. Indeed, it was previously shown that TGFBI inhibits osteogenesis and mineralization of cultured chondrocytes [30-32]. On the other hand, in immature chondrocytes isolated from femoral and tibial epiphyses of 3-day-old mice, TGFBI was downregulated in OA-like conditions. In mouse embryos (E16.5 to E18.5), TGFBI is expressed in proliferating chondrocytes and in primary endochondral ossification centres during joint cartilage formation, where it may interact with cells and extracellular matrix molecules, thus playing a role in tissue morphogenesis [33-35]. In 3-day-old mice, cartilage is predominantly pre-hypertrophic and hypertrophic, consistent with high TGFBI expression, as observed during embryogenesis. We previously reported that TGFBI is required at

the early stages of chondrogenic differentiation of MSCs, and is then downregulated in mineralized hypertrophic chondrocytes [21]. The present study brings evidence that besides promoting endochondral ossification and inhibiting mineralization during *in vitro* differentiation of mature osteoblasts or chondrocytes, TGFBI deregulation in joint tissues might contribute to OA.

TGFBI is a paralogue of periostin (*POSTN*), the only other member of the TGFBI family. The two genes have a similar domain structure, although *TGFBI* is shorter and lacks the C-terminal domain that is subjected to alternative splicing in *POSTN* [36, 37]. Both genes have important overlapping functions in cell adhesion, migration, proliferation, and apoptosis. In cancer, they display dual roles, acting as tumour suppressors or promoters, depending on the tumour environment. POSTN levels in serum and synovial fluid are associated with OA incidence and progression [38, 39], and its expression is higher in mouse and human bone and cartilage [40, 41]. Importantly, the higher chondroprotective effect in OA mice of FRA-1-overexpressing adipose-derived stromal cells compared with wild type cells has been associated with increased POSTN expression [42]. We recently reported TGFBI upregulation in bone and cartilage from patients and mice with OA [21]. Based on the similarity of functions and expression in OA, all these data suggest a possible common regulation of POSTN and TGFBI in OA and identify these two molecules as important players in joint homeostasis. In agreement, the present study demonstrated the lower *in vivo* therapeutic efficiency of siTGFBI-hMSCs that mimic the lower TGFBI expression of hMSCs from patients with OA. Interestingly, siTGFBI-hMSCs could not reduce osteophyte calcification in CIOA mice (data not shown), further supporting a probable inhibitory role of TGFBI on mineralization *in vivo*. TGFβ pathway deregulation in MSCs was

previously associated with OA onset and/or maintenance [20]. Here, we present further evidence that TGFBI deregulation in OA MSCs impairs their therapeutic chondroprotective function and might affect their physiologic role in cartilage and bone homeostasis.

We provided evidence that EVs released by mMSCs and hMSCs contain both TGFBI mRNA and protein, underlining a plausible common mechanism of action. Usually, EVs act on target cells after their internalization mediated by fusion of their membrane with the cell plasma membrane or after uptake. After uptake, EVs are addressed to the canonical endosomal pathway and can be targeted to lysosomes and degraded, or can discharge their cargo in the cytosol by fusion with the endosomal membrane [43]. A possible transfer of EVs to the plasma membrane for release might also occur. In our conditions, we could not detect the presence of human *TGFBI* mRNA in murine chondrocytes after 1 day of co-culture with hMSCs (data not shown), possibly because after uptake, the amount of *TGFBI* mRNA released in chondrocytes might have been too low to be detected, or rapidly degraded or translated into proteins. Further investigations are needed to determine the fate of EV cargoes in chondrocytes or synovial cells in the joint. Nevertheless, we previously demonstrated that IA injection of small-size and large size mMSC-EVs can protect mice from developing CIOA to a similar extent as mMSCs, suggesting that TGFBI mRNA and protein contained in EVs might play an important role [27]. The relative contribution of soluble TGFBI and EV-contained TGFBI needs to be investigated.

One of the main roles of TGFBI is to mediate cell adhesion and migration by acting as a linker that connects various matrix molecules and favours cell-collagen interactions. This has been shown mainly in tumour cells where TGFBI can act either as tumour promoter by

increasing cancer cell invasiveness, or as a tumour suppressor by inhibiting cell adhesion leading to inhibition of cell proliferation and migration [44]. TGFBI also increases cell survival and proliferation during gastrointestinal tract tumorigenesis via activation of the FAK/AKT signalling pathway [45]. Moreover, TGFBI expression is a predictor of survival in patients with lung squamous cell carcinoma [46]. However, its physiological role is still unclear. Here, we demonstrated that TGFBI decreases chondrocyte adhesion and increases their proliferation. Therefore, TGFBI secreted by MSCs might mediate its therapeutic effect in joint tissues via a pro-survival and pro-anabolic role on chondrocytes.

TGFBI could also have an anti-inflammatory effect through its negative regulation of Toll like receptor-induced inflammation. For instance, TGFBI expression was increased in peripheral blood mononuclear cells in a model of lipopolysaccharide-induced endotoxin tolerance, resulting in lower activation of inflammatory actors, such as nuclear factor-κB, TNF-α and nitric oxide [47]. Moreover, a significant correlation has been observed between three single nucleotide polymorphisms in the *TGFBI* gene and type 1 diabetes, and TGFBI expression is lower in pancreatic islets from diabetic subjects. Interestingly, TGFBI can inhibit T-cell activation markers (CD44 and CD69) and the production of cytotoxic molecules, such as granzyme B and interferon-γ [48]. In addition, TGFBI-treated diabetogenic T cells cannot induce type 1 diabetes upon transfer in wild type mice, suggesting that TGFBI expression in pancreatic islets might contribute as a protective shield against cytotoxic T-cell attack. Our data indicated that TGFBI plays a role in MSC anti-inflammatory function and contributes to T lymphocyte proliferation inhibition. Therefore, the hypothesis that TGFBI released by hMSCs might exert an anti-inflammatory function in OA should be investigated *in vivo*.

Altogether, the present study highlights TGFBI role in hMSC chondroprotective effect in OA by inhibiting cartilage and bone degradation, while limiting calcification and osteophyte formation. Besides deciphering the mechanisms underlying hMSC therapeutic effect, it suggests the possibility of targeting TGFBI for therapeutic intervention.

ACKNOWLEDGEMENTS

We gratefully acknowledge funding support from the Inserm Institute, the University of Montpellier, the Agence Nationale pour la Recherche for support of the national infrastructure: "ECELLFRANCE: Development of a national adult mesenchymal stem cell based therapy platform" (ANR-11-INSB-005). The study was also supported by Arthritis R&D through the program "ROAD: Research on OsteoArthritis Diseases" and the European Union Horizon 2020 Programme (project ADIPOA2, grant agreement no: 643809). The materials presented and views expressed here are the responsibility of the authors only. The EU Commission takes no responsibility for any use made of the information set out. We thank the Réseau d'Histologie Expérimentale de Montpellier histology facility for tissue processing. We also thank the "SMARTY platform and Network of Animal facilities of Montpellier".

CONFLICT OF INTEREST

The authors disclose any financial or personal conflict of interest.

DATA AVAILABILITY

All experimental data required to reproduce the findings from this study will be made available to interested investigators.

AUTHOR CONTRIBUTIONS

DN, CJ designed the experiments. Experimental work was performed by MR, MM, KT, PR, DN. MR, MM, KT, PR, CJ, DN analysed the data and prepared the manuscript. All authors have contributed to writing or revising the manuscript and final approval.

REFERENCES

[1] R. Hass, C. Kasper, S. Bohm, R. Jacobs, Different populations and sources of human mesenchymal stem cells (MSC): A comparison of adult and neonatal tissue-derived MSC, Cell Commun Signal 9 (2011) 12.
[2] M. Dominici, K. Le Blanc, I. Mueller, I. Slaper-Cortenbach, F. Marini, D. Krause, R. Deans, A. Keating, D. Prockop, E. Horwitz, Minimal criteria for defining multipotent mesenchymal stromal cells. The International Society for Cellular Therapy position statement, Cytotherapy 8(4) (2006) 315-7.
[3] J. Galipeau, M. Krampera, J. Barrett, F. Dazzi, R.J. Deans, J. DeBruijn, M. Dominici, W.E. Fibbe, A.P. Gee, J.M. Gimble, P. Hematti, M.B. Koh, K. LeBlanc, I. Martin, I.K. McNiece, M. Mendicino, S. Oh, L. Ortiz, D.G. Phinney, V. Planat, Y. Shi, D.F. Stroncek, S. Viswanathan, D.J. Weiss, L. Sensebe, International Society for Cellular Therapy perspective on immune functional assays for mesenchymal stromal cells as potency release criterion for advanced phase clinical trials, Cytotherapy 18(2) (2016) 151-9.
[4] S. Cosenza, M. Ruiz, M. Maumus, C. Jorgensen, D. Noel, Pathogenic or Therapeutic Extracellular Vesicles in Rheumatic Diseases: Role of Mesenchymal Stem Cell-Derived Vesicles, Int J Mol Sci 18(4) (2017).
[5] C. Bouffi, C. Bony, G. Courties, C. Jorgensen, D. Noel, IL-6-dependent PGE2 secretion by mesenchymal stem cells inhibits local inflammation in experimental arthritis, PLoS One 5(12) (2010) e14247.
[6] P. Luz-Crawford, F. Djouad, K. Toupet, C. Bony, M. Franquesa, M.J. Hoogduijn, C. Jorgensen, D. Noel, Mesenchymal Stem Cell-Derived Interleukin 1 Receptor Antagonist Promotes Macrophage Polarization and Inhibits B Cell Differentiation, Stem Cells 34(2) (2016) 483-92.
[7] P. Luz-Crawford, G. Tejedor, A.L. Mausset-Bonnefont, E. Beaulieu, E.F. Morand, C. Jorgensen, D. Noel, F. Djouad, Gilz governs the therapeutic potential of mesenchymal stem cells by inducing a switch from pathogenic to regulatory Th17 cells, Arthritis Rheumatol 67(6) (2015) 1514-24.
[8] M. Maumus, C. Manferdini, K. Toupet, P. Chuchana, L. Casteilla, M. Gachet, C. Jorgensen, G. Lisignoli, D. Noel, Thrombospondin-1 Partly Mediates the Cartilage Protective Effect of Adipose-Derived Mesenchymal Stem Cells in Osteoarthritis, Front Immunol 8 (2017) 1638.
[9] A. Mobasheri, M. Batt, An update on the pathophysiology of osteoarthritis, Ann Phys Rehabil Med 59(5-6) (2016) 333-339.
[10] F. Berenbaum, T.M. Griffin, R. Liu-Bryan, Review: Metabolic Regulation of Inflammation in Osteoarthritis, Arthritis Rheumatol 69(1) (2017) 9-21.
[11] M.B. Goldring, F. Berenbaum, Emerging targets in osteoarthritis therapy, Curr Opin Pharmacol 22 (2015) 51-63.
[12] G. Desando, C. Cavallo, F. Sartoni, L. Martini, A. Parrilli, F. Veronesi, M. Fini, R. Giardino, A. Facchini, B. Grigolo, Intra-articular delivery of adipose derived stromal cells attenuates osteoarthritis progression in an experimental rabbit model, Arthritis Res Ther 15(1) (2013) R22.
[13] J.M. Murphy, D.J. Fink, E.B. Hunziker, F.P. Barry, Stem cell therapy in a caprine model of osteoarthritis, Arthritis Rheum 48(12) (2003) 3464-74.
[14] M. Ter Huurne, R. Schelbergen, R. Blattes, A. Blom, W. de Munter, L.C. Grevers, J. Jeanson, D. Noel, L. Casteilla, C. Jorgensen, W. van den Berg, P.L. van Lent, Antiinflammatory and chondroprotective effects of intraarticular injection of adipose-derived stem cells in experimental osteoarthritis, Arthritis Rheum 64(11) (2012) 3604-13.
[15] M. Ruiz, S. Cosenza, M. Maumus, C. Jorgensen, D. Noel, Therapeutic application of mesenchymal stem cells in osteoarthritis, Expert Opin Biol Ther 16(1) (2015) 33-42.

[16] M.M. Schimke, S. Marozin, G. Lepperdinger, Patient-Specific Age: The Other Side of the Coin in Advanced Mesenchymal Stem Cell Therapy, Front Physiol 6 (2015) 362.
[17] N. Baker, L.B. Boyette, R.S. Tuan, Characterization of bone marrow-derived mesenchymal stem cells in aging, Bone 70 (2015) 37-47.
[18] G. Zhai, J. Dore, P. Rahman, TGF-beta signal transduction pathways and osteoarthritis, Rheumatol Int 35(8) (2015) 1283-92.
[19] P.M. van der Kraan, The changing role of TGFbeta in healthy, ageing and osteoarthritic joints, Nat Rev Rheumatol 13(3) (2017) 155-163.
[20] G. Zhen, C. Wen, X. Jia, Y. Li, J.L. Crane, S.C. Mears, F.B. Askin, F.J. Frassica, W. Chang, J. Yao, J.A. Carrino, A. Cosgarea, D. Artemov, Q. Chen, Z. Zhao, X. Zhou, L. Riley, P. Sponseller, M. Wan, W.W. Lu, X. Cao, Inhibition of TGF-beta signaling in mesenchymal stem cells of subchondral bone attenuates osteoarthritis, Nat Med 19(6) (2013) 704-12.
[21] M. Ruiz, M. Maumus, G. Fonteneau, Y.M. Pers, R. Ferreira, L. Dagneaux, C. Delfour, X. Houard, F. Berenbaum, F. Rannou, C. Jorgensen, D. Noel, TGFbetai is involved in the chondrogenic differentiation of mesenchymal stem cells and is dysregulated in osteoarthritis, Osteoarthritis Cartilage 27(3) (2019) 493-503.
[22] A.T. Maria, K. Toupet, M. Maumus, G. Fonteneau, A. Le Quellec, C. Jorgensen, P. Guilpain, D. Noel, Human adipose mesenchymal stem cells as potent anti-fibrosis therapy for systemic sclerosis, J Autoimmun 70 (2016) 31-9.
[23] S. Cosenza, K. Toupet, M. Maumus, P. Luz-Crawford, O. Blanc-Brude, C. Jorgensen, D. Noel, Mesenchymal stem cells-derived exosomes are more immunosuppressive than microparticles in inflammatory arthritis, Theranostics 8(5) (2018) 1399-1410.
[24] H. Stanton, S.B. Golub, F.M. Rogerson, K. Last, C.B. Little, A.J. Fosang, Investigating ADAMTS-mediated aggrecanolysis in mouse cartilage, Nat Protoc 6(3) (2011) 388-404.
[25] M. Gosset, F. Berenbaum, S. Thirion, C. Jacques, Primary culture and phenotyping of murine chondrocytes, Nat Protoc 3(8) (2008) 1253-60.
[26] S. Domergue, C. Bony, M. Maumus, K. Toupet, E. Frouin, V. Rigau, M.C. Vozenin, G. Magalon, C. Jorgensen, D. Noel, Comparison between Stromal Vascular Fraction and Adipose Mesenchymal Stem Cells in Remodeling Hypertrophic Scars, PLoS One 11(5) (2016) e0156161.
[27] S. Cosenza, M. Ruiz, K. Toupet, C. Jorgensen, D. Noel, Mesenchymal stem cells derived exosomes and microparticles protect cartilage and bone from degradation in osteoarthritis, Sci Rep 7(1) (2017) 16214.
[28] M. Ruiz, M. Maumus, G. Fonteneau, Y.M. Pers, R. Ferreira, L. Dagneaux, C. Delfour, X. Houard, F. Berenbaum, F. Rannou, C. Jorgensen, D. Noel, TGFbetai is involved in the chondrogenic differentiation of mesenchymal stem cells and is dysregulated in osteoarthritis, Osteoarthritis Cartilage (2018).
[29] K. Toupet, M. Maumus, P. Luz-Crawford, E. Lombardo, J. Lopez-Belmonte, P. van Lent, M.I. Garin, W. van den Berg, W. Dalemans, C. Jorgensen, D. Noel, Survival and biodistribution of xenogenic adipose mesenchymal stem cells is not affected by the degree of inflammation in arthritis, PLoS One 10(1) (2015) e0114962.
[30] M.J. Lee, S.C. Heo, S.H. Shin, Y.W. Kwon, E.K. Do, D.S. Suh, M.S. Yoon, J.H. Kim, Oncostatin M promotes mesenchymal stem cell-stimulated tumor growth through a paracrine mechanism involving periostin and TGFBI, Int J Biochem Cell Biol 45(8) (2013) 1869-77.
[31] J. Ren, P. Jin, M. Sabatino, A. Balakumaran, J. Feng, S.A. Kuznetsov, H.G. Klein, P.G. Robey, D.F. Stroncek, Global transcriptome analysis of human bone marrow stromal cells (BMSC) reveals proliferative, mobile and interactive cells that produce abundant extracellular matrix proteins, some of which may affect BMSC potency, Cytotherapy 13(6) (2011) 661-74.

[32] R. Bhushan, J. Grunhagen, J. Becker, P.N. Robinson, C.E. Ott, P. Knaus, miR-181a promotes osteoblastic differentiation through repression of TGF-beta signaling molecules, Int J Biochem Cell Biol 45(3) (2013) 696-705.
[33] J.W. Ferguson, M.F. Mikesh, E.F. Wheeler, R.G. LeBaron, Developmental expression patterns of Beta-ig (betaIG-H3) and its function as a cell adhesion protein, Mech Dev 120(8) (2003) 851-64.
[34] M.S. Han, J.E. Kim, H.I. Shin, I.S. Kim, Expression patterns of betaig-h3 in chondrocyte differentiation during endochondral ossification, Exp Mol Med 40(4) (2008) 453-60.
[35] S. Ohno, T. Doi, S. Tsutsumi, Y. Okada, K. Yoneno, Y. Kato, K. Tanne, RGD-CAP ((beta)ig-h3) is expressed in precartilage condensation and in prehypertrophic chondrocytes during cartilage development, Biochim Biophys Acta 1572(1) (2002) 114-22.
[36] X. Song, L. Cai, Y. Li, J. Zhu, P. Jin, L. Chen, F. Ma, Identification and characterization of transforming growth factor beta induced gene (TGFBIG) from Branchiostoma belcheri: insights into evolution of TGFBI family, Genomics 103(1) (2014) 147-53.
[37] D.F. Mosher, M.W. Johansson, M.E. Gillis, D.S. Annis, Periostin and TGF-beta-induced protein: Two peas in a pod?, Crit Rev Biochem Mol Biol 50(5) (2015) 427-39.
[38] S. Honsawek, V. Wilairatana, W. Udomsinprasert, P. Sinlapavilawan, N. Jirathanathornnukul, Association of plasma and synovial fluid periostin with radiographic knee osteoarthritis: Cross-sectional study, Joint Bone Spine 82(5) (2015) 352-5.
[39] J.C. Rousseau, E. Sornay-Rendu, C. Bertholon, P. Garnero, R. Chapurlat, Serum periostin is associated with prevalent knee osteoarthritis and disease incidence/progression in women: the OFELY study, Osteoarthritis Cartilage 23(10) (2015) 1736-42.
[40] C.H. Chou, C.C. Wu, I.W. Song, H.P. Chuang, L.S. Lu, J.H. Chang, S.Y. Kuo, C.H. Lee, J.Y. Wu, Y.T. Chen, V.B. Kraus, M.T. Lee, Genome-wide expression profiles of subchondral bone in osteoarthritis, Arthritis Res Ther 15(6) (2013) R190.
[41] R.F. Loeser, A.L. Olex, M.A. McNulty, C.S. Carlson, M.F. Callahan, C.M. Ferguson, J. Chou, X. Leng, J.S. Fetrow, Microarray analysis reveals age-related differences in gene expression during the development of osteoarthritis in mice, Arthritis Rheum 64(3) (2012) 705-17.
[42] K. Schwabe, M. Garcia, K. Ubieta, N. Hannemann, B. Herbort, J. Luther, D. Noel, C. Jorgensen, L. Casteilla, J.P. David, M. Stock, M. Herrmann, G. Schett, A. Bozec, Inhibition of Osteoarthritis by Adipose-Derived Stromal Cells Overexpressing Fra-1 in Mice, Arthritis Rheumatol 68(1) (2016) 138-51.
[43] G. van Niel, G. D'Angelo, G. Raposo, Shedding light on the cell biology of extracellular vesicles, Nat Rev Mol Cell Biol 19(4) (2018) 213-228.
[44] M.P. Ween, M.K. Oehler, C. Ricciardelli, Transforming growth Factor-Beta-Induced Protein (TGFBI)/(betaig-H3): a matrix protein with dual functions in ovarian cancer, Int J Mol Sci 13(8) (2012) 10461-77.
[45] B. Han, H. Cai, Y. Chen, B. Hu, H. Luo, Y. Wu, J. Wu, The role of TGFBI (betaig-H3) in gastrointestinal tract tumorigenesis, Mol Cancer 14 (2015) 64.
[46] M.J. Pajares, J. Agorreta, E. Salvo, C. Behrens, Wistuba, II, L.M. Montuenga, R. Pio, A. Rouzaut, TGFBI expression is an independent predictor of survival in adjuvant-treated lung squamous cell carcinoma patients, Br J Cancer 110(6) (2014) 1545-51.
[47] Y. Yang, H. Sun, X. Li, Q. Ding, P. Wei, J. Zhou, Transforming Growth Factor Beta-Induced Is Essential for Endotoxin Tolerance Induced by a Low Dose of Lipopolysaccharide in Human Peripheral Blood Mononuclear Cells, Iran J Allergy Asthma Immunol 14(3) (2015) 321-30.
[48] M. Patry, R. Teinturier, D. Goehrig, C. Zetu, D. Ripoche, I.S. Kim, P. Bertolino, A. Hennino, betaig-h3 Represses T-Cell Activation in Type 1 Diabetes, Diabetes 64(12) (2015) 4212-9.

Figure legends

Figure 1. Modulation of TGFBI expression in mouse tissues and in *in vitro* OA-like models. A) *Tgfbi* mRNA expression in the indicated tissues from 3-day-old healthy mice. B) *Tgfbi* mRNA expression in the indicated tissues from adult mice. C) *Tgfbi* mRNA expression in epiphyses from adult healthy mice and after OA induction. D) Scheme showing the OA-like model based on incubation of adult femoral head explants with IL1β. E) RT-qPCR analysis of different chondrocyte markers and TGFBI in control (NT, not treated with IL1β) and OA-like femoral head explants (IL1β). Glycosaminoglycan (GAG) quantification in femoral head explants, and GAG release in the culture medium from NT and IL1β-treated samples after 3 days. F) Scheme explaining the generation of OA-like chondrocytes by incubation with IL1β. G) RT-qPCR analysis of different chondrocyte and inflammatory markers and of TGFBI in control (NT, not treated with IL1β) and OA-like chondrocytes (IL1β). Each dot represents one biological replicate, and results are expressed as the mean ± SEM. Groups were compared with the Kruskal-Wallis test followed by the Dunn's multiple comparisons test in (A-B), the Mann-Whitney test in (C, E, G), or the Wilcoxon signed-rank test to compare NT and IL1β-treated samples (dotted line) (E, G). *: $p<0.05$; **: $p<0.01$; ***: $p<0.001$, and ****: $p<0.0001$.

Figure 2. Effect of mMSCs and hMSCs on chondrocyte gene expression in the *in vitro* OA-like models. A) Glycosaminoglycan (GAG) quantification in the supernatant of OA-like femoral head explants (IL1β) after 3 days of co-culture or not with mMSCs (left). RT-qPCR analysis of the chondrocyte markers *Col2a1* (middle) and *Acan* (right) in control (NT, not treated with IL1β)

and OA-like femoral head explants (IL1β) after 3 days of co-culture or not with mMSCs (n=5-10 biological replicates). B) RT-qPCR analysis of different chondrocyte and inflammatory markers in control (NT, not treated with IL1β) and OA-like chondrocytes (IL1β) incubated or not with mMSC conditioned medium (mMSC-CM). C) RT-qPCR analysis of different chondrocyte and inflammatory markers in control (NT) and OA-like chondrocytes (IL1β) co-cultured or not with mMSCs. D) RT-qPCR analysis of different chondrocyte and inflammatory markers in control (NT) and OA-like chondrocytes (IL1β) co-cultured or not with hMSCs. Each dot represents one biological replicate, and results are expressed as the mean ± SEM. Two groups were compared with the Mann-Whitney test (A), and samples were compared to OA-like chondrocytes (IL1β; set to 1) with the Wilcoxon signed-rank test (dotted line) (B-D). *: $p<0.05$; **: $p<0.01$; ***: $p<0.001$, and ****: $p<0.0001$.

Figure 3. Effect of TGFβ3-primed mMSCs and hMSCs on chondrocyte gene expression in *in vitro* OA-like models. A) RT-qPCR analysis of *Tgfbi* in mMSCs primed (TGFβ3) or not (NT) with TGFβ3 (n=17/group). B) RT-qPCR analysis of *TGFBI* (left panel; n=11 biological replicates) and quantification of TGFBI in the supernatant (right panel, n=4 biological replicates) of control (NT) and TGFβ3-primed hMSCs. C-D) RT-qPCR analysis of chondrocyte and inflammatory markers in control (NT, not treated with IL1β) and OA-like chondrocytes (IL1β) incubated or not with conditioned medium from TGFβ3-primed mMSCs (mMSC-CM*) (C), or co-cultured or not with TGFβ3-primed mMSCs (mMSC*) (D). E) RT-qPCR analysis of chondrocyte and inflammatory markers in control (NT) and OA-like chondrocytes (IL1β) co-cultured or not with TGFβ3-primed hMSCs (hMSC*). Each dot represents one biological replicate, and results are expressed as the

mean ± SEM. The Mann-Whitney test was used to compare two groups (A), and the Wilcoxon signed-rank test to compare samples to IL1β-treated chondrocytes (set to 1; dotted line) (C-E). *: $p<0.05$; **: $p<0.01$; ***: $p<0.001$ or ****: $p<0.0001$.

Figure 4. Effect of TGFBI silencing in mMSCs and hMSCs on co-cultured OA-like chondrocytes. A) RT-qPCR analysis of *Tgfbi* in mMSCs transfected with control (siCT) or anti-TGFBI siRNAs (siTBI) and of chondrocyte markers in control (NT, not treated with IL1β) and OA-like chondrocytes (IL1β) co-cultured or not with siCT- or siTBI-transfected mMSCs (n=8 biological replicates). B) RT-qPCR analysis of *Tgfbi* in siCT- and siTBI transfected mMSCs and of chondrocyte genes in control (NT) and OA-like chondrocytes (IL1β) co-cultured or not with siCT- or siTBI-transfected TGFβ3-primed mMSCs (mMSCs*; n=12 biological replicates). C) RT-qPCR analysis of *TGFBI* in siCT- and siTBI-transfected hMSCs and of chondrocyte genes in control (NT) and OA-like chondrocytes (IL1β) co-cultured or not with siCT- or siTBI-transfected TGFβ3-primed hMSCs (hMSCs*; n=8 biological replicates). Results are expressed as the mean ± SEM. The Wilcoxon signed-rank test was used to compare OA-like chondrocytes (IL1β) in different conditions to OA-like chondrocytes co-cultured with siCT-mMSCs or hMSCs (set to 1; dotted line). *: $p<0.05$; **: $p<0.01$.

Figure 5. Effect of siTGFBI-hMSCs in the collagenase-induced osteoarthritic (CIOA) murine model. A) Histological images of healthy (H) mice and CIOA mice not treated (NT) or treated with hMSCs transfected with control (siCT) or anti-TGFBI (siTBI) mRNAs. B) OA score of histological sections of knee joints of the mice described in A. C) Histomorphometric analysis of

3D images of cartilage by CLSM. D) Representative 3D reconstructed images of medial tibial cartilage after CLSM analysis; on the left, colour code for cartilage thickness. E) Representative 3D reconstructed images of the sub-chondral bone surface in tibias after micro-CT analysis. F) Histomorphometric analysis of 3D images of sub-chondral bone: thickness and bone surface/bone volume (BS/BV) parameters (n=15/group). G) Histomorphometric analysis (volume and surface) of mineralized tissues in joints. H) Representative 3D reconstructed images of mouse knee joints after micro-CT analysis showing mineralized menisci and external ligaments. Results are expressed as the mean ± SEM; *: $p<0.05$; ****: $p<0.0001$ (Mann-Whitney test; n=23 mice/group from 2 independent experiments).

Figure 6. Functional effect of TGFBI. A) Proliferation of chondrocytes on plates coated with recombinant hTGFBI, expressed as fold change compared with cells cultured on plates coated with PBS (NT). B) Adhesion of chondrocytes on plates coated with PBS (NT) or recombinant hTGFBI, expressed as the cell number fold-change relative to NT at the indicated time points after seeding normalized (n=9 biological replicates). C) Proliferation of concanavalin A-activated mouse splenocytes co-cultured or not with hMSCs transfected with control (siCT) or anti-siTGFBI siRNAs at two ratios (1:10 or 1:20, hMSCs:splenocytes) (n=7 biological replicates). D) Number and median size of extracellular vesicles from hMSCs (hMSC-EVs) by nano-particle tracking analysis. E) Representative histograms of hMSC-EV surface markers by flow cytometry. F) TGFBI protein expression in hMSC-EVs and in hMSCs normalized to the total protein amount. G) Expression of *TGFBI* mRNA in hMSCs and hMSC-EVs as expressed as Ct value. H) Expression of *TGFBI* mRNA in hMSCs and hMSC-EVs as well as in mMSCs, mMSC-ssEVs (small-size EVs) and

mMSC-lsEVs (large-size EVs), expressed as Ct value. Each dot represents a biological replicate and results are expressed as the mean ± SEM. *: $p<0.05$; ****: $p<0.0001$ (Wilcoxon signed-rank test in (A) and Mann-Whitney test in (B-C).

Table
Click here to download Table: Table 1.docx

Table 1: List of primer sequences for RT-qPCR analysis

Gene	Sequence forward	Sequence reverse
mADAMTS5	CTGCCTTCAAGGCAAATGTGTGG	CAATGGCGGTAGGCAAACTGC
mAGG	GCGAGTCCAACTCTTCAAGC	GAAGTAGCAGGGGATGGTGA
mCOL2B	CTGGTGCTGCTGACGCT	GCCCTAATTTTCGGGCAT
mCOX2	GCATTCTTTGCCCAGCACTT	AGACCAGGCACCAGACCAAAGA
mIL6	TGGGACTGATGCTGGTGACA	TTCCACGATTTCCCAGAGAACA
mINOS	CCTTGTTCAGCTACGCCTTC	GCTTGTCACCACCAGCAGTA
mMCP1	TGCAGGTCCCTGTCATGCTT	TCCTTCTTGGGGTCAGCACA
mMMP13	TCTGGATCACTCCAAGGACC	ATCAGGAAGCATGAAATGGC
mTGFBI	ACCATCAACGGGAAGGCTGTCA	AGCCAGCTCAAGCAGTGTCTTG
mTNFalpha	AGCCCACGTCGTAGCAAACCA	TGTCTTTGAGATCCATGCCGTTGGC
hTGFBI	GGACATGCTCACTATCAACGGG	CTGTGGACACATCAGACTCTGC

Figure 1

Click here to download high resolution image

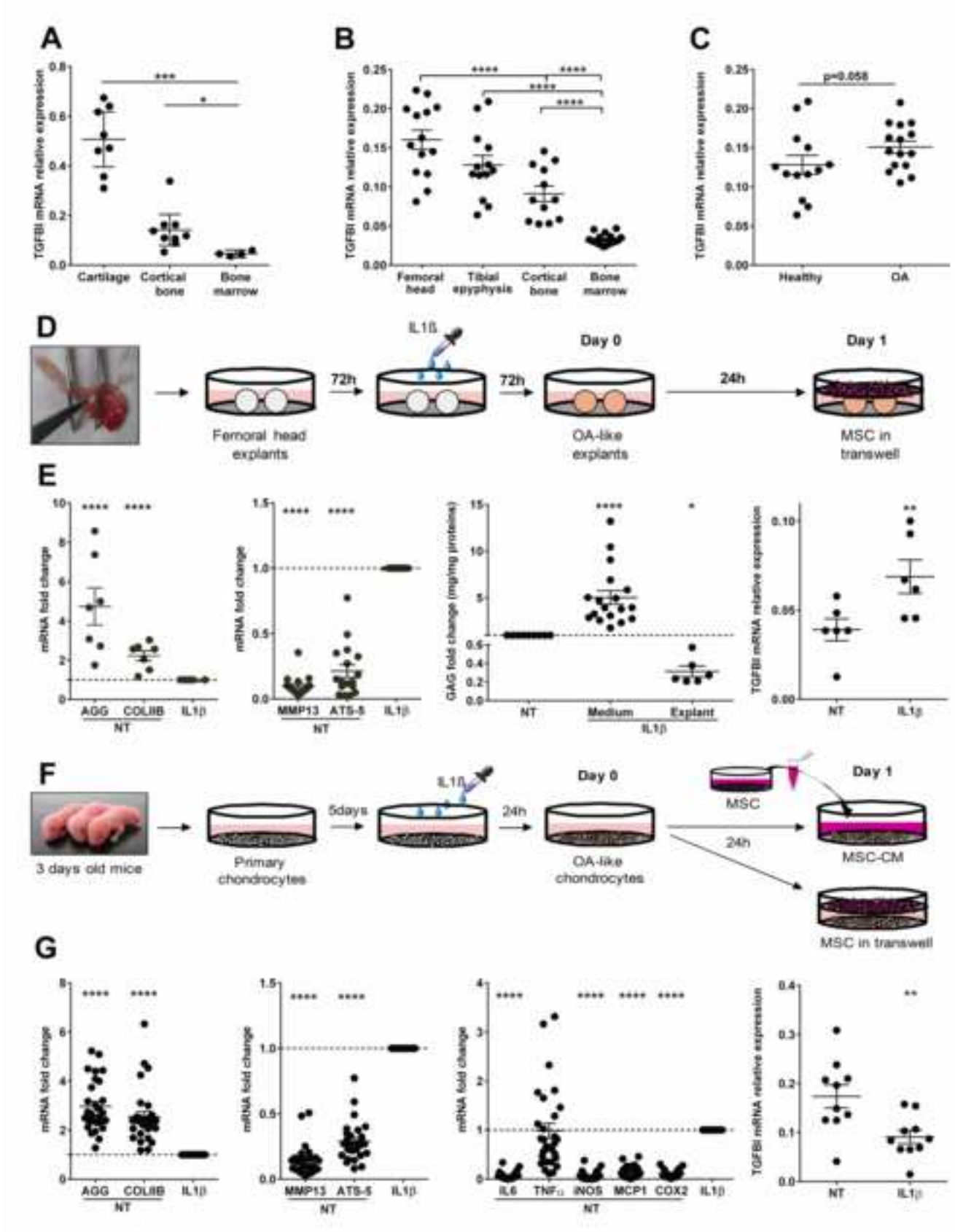

Figure 2

Click here to download high resolution image

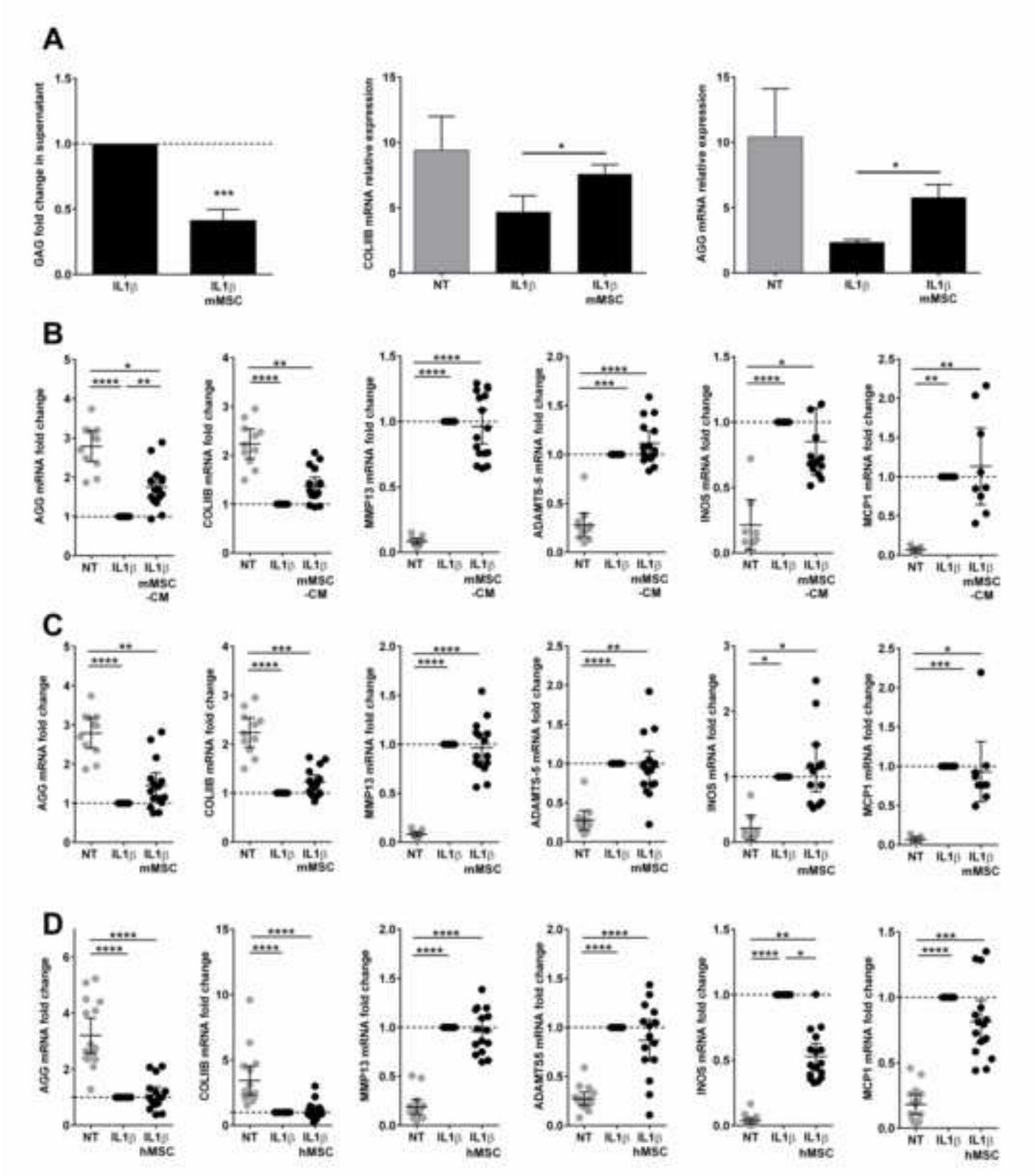

Figure 3

Click here to download high resolution image

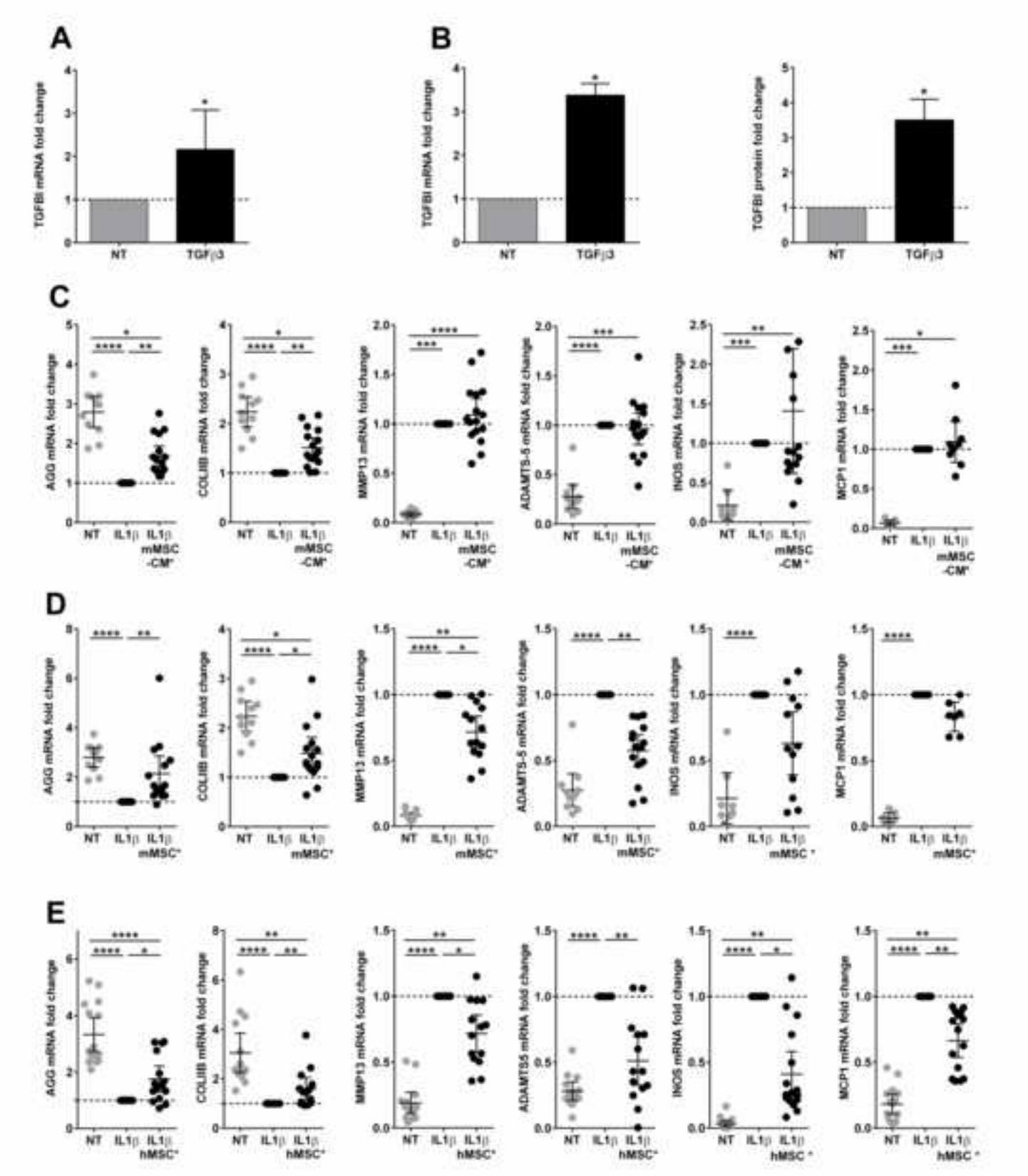

Figure 4
Click here to download high resolution image

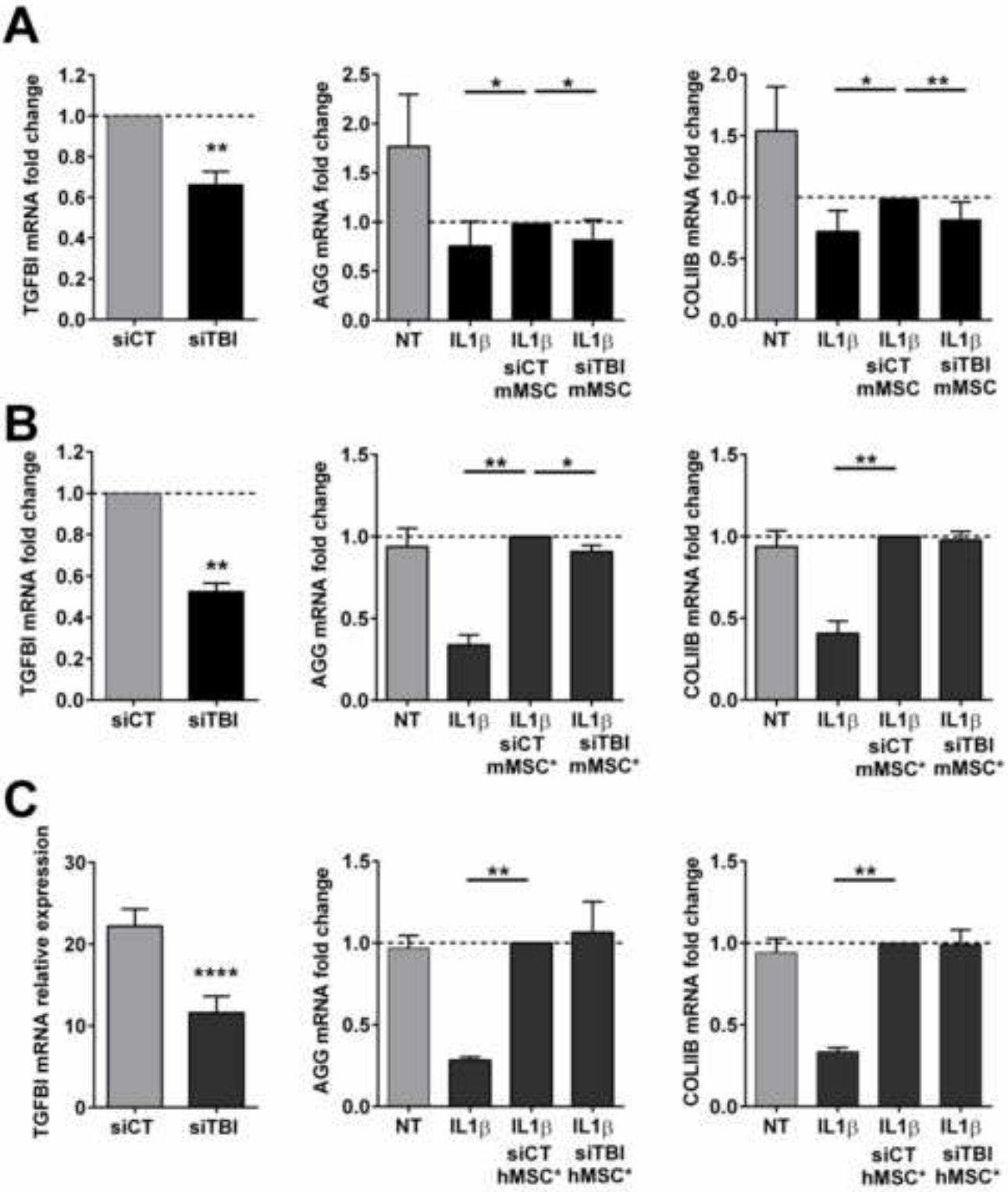

Figure 5

Click here to download high resolution image

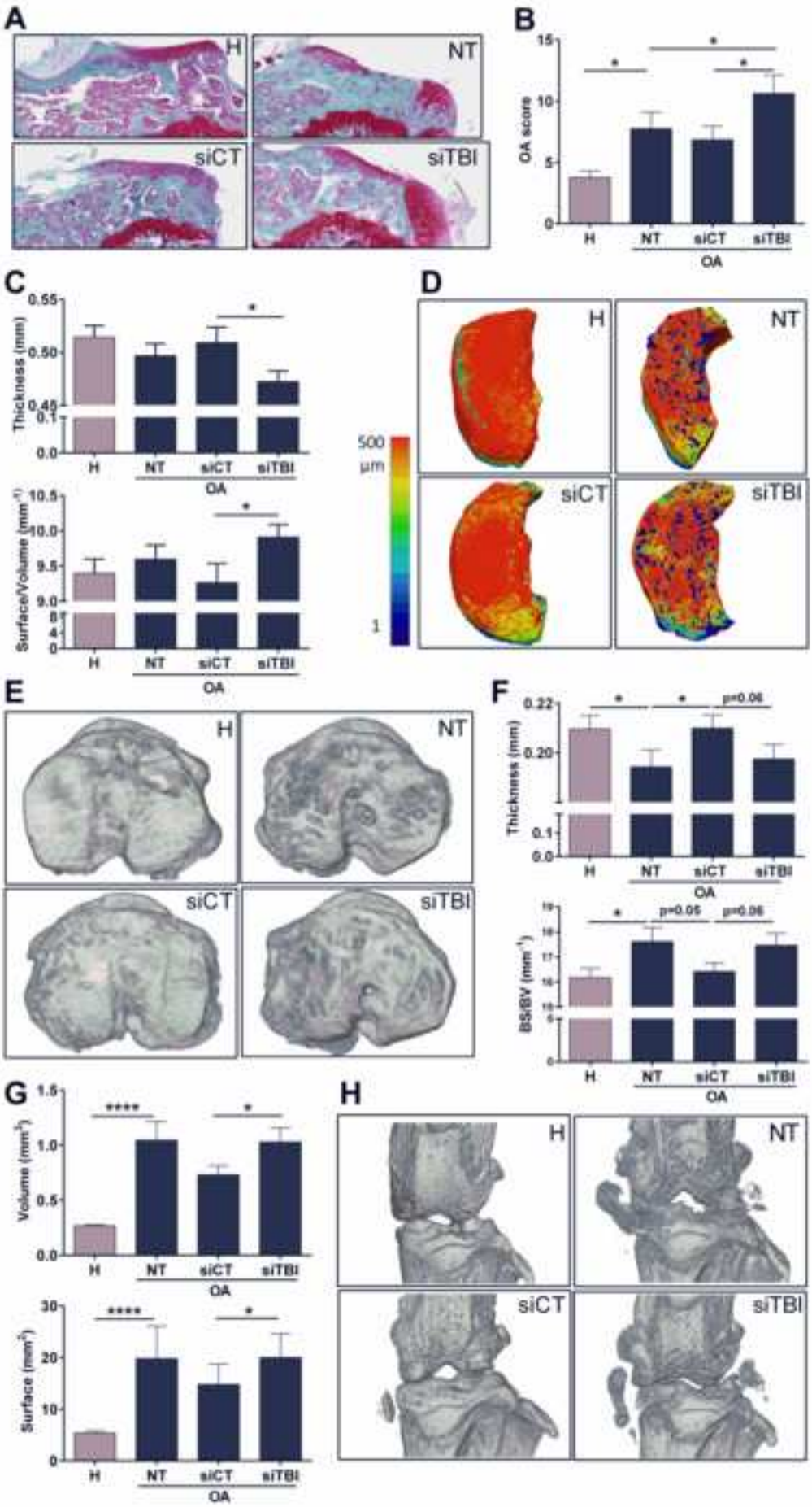

Figure 6
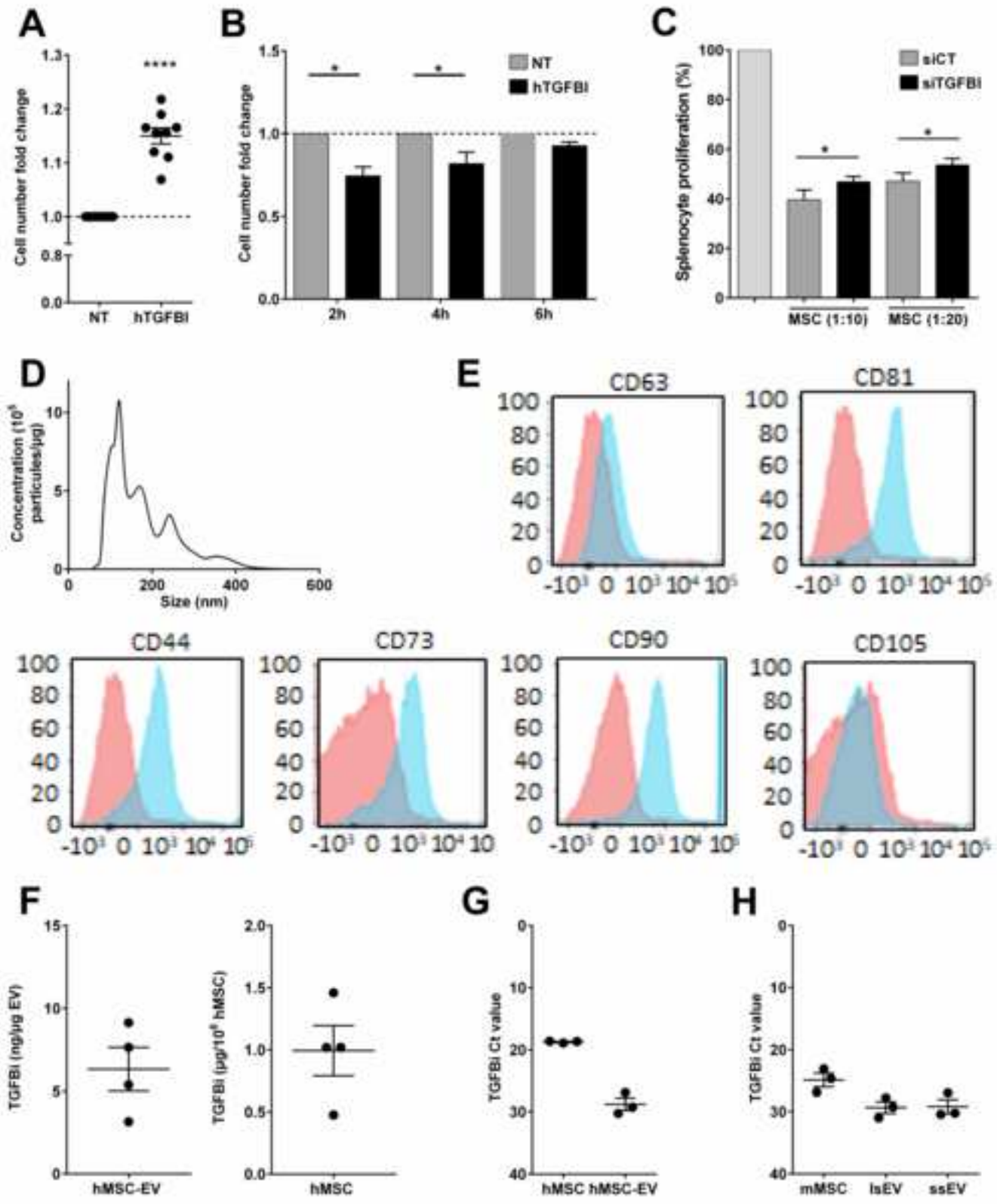
Click here to download high resolution image